ACS APPLIED MATERIALS & INTERFACES

Research Article

www.acsami.org

Ordered Array of Gold Semishells on TiO_2 Spheres: An Ultrasensitive and Recyclable SERS Substrate

Xianglin Li,[†] Hailong Hu,[†] Dehui Li,[†] Zexiang Shen,[†] Qihua Xiong,[†] Shuzhou Li,[‡] and Hong Jin Fan[†,*]

[†]Division of Physics and Applied Physics, School of Physical and Mathematical Sciences, Nanyang Technological University, 637371, Singapore

[‡]School of Materials Science and Engineering, Nanyang Technological University, 639798, Singapore

ABSTRACT: Ordered array of Au semishells on TiO_2 spheres with controlled size are prepared by combining the nanosphere self-assembly and atomic layer deposition (ALD). This ordered 2-D structure with designed array of metal nanogaps can be used as an ultrasensitive surface-enhanced Raman scattering (SERS) substrate with high reproducibility and stability. More importantly, the SERS substrates are recyclable, as enabled by their self-cleaning function due to the TiO_2 photocatalytic degradation of the target molecules. The high SERS sensitivity and recyclability are demonstrated by the detection of Rhodamine 6G (R6G) and brilliant cresyl blue (BCB) molecules. As both the nanosphere lithography and ALD are scalable processes, such 2-D ordered substrates may find applications in chemical sensing.

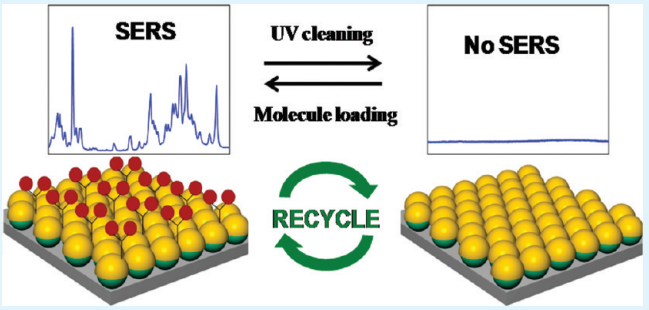

KEYWORDS: *Surface-enhanced Raman scattering, semishell, ordered array, TiO_2, recyclable, photocatalytic degradation*

1. INTRODUCTION

As a powerful spectroscopic technique, surface-enhanced Raman scattering (SERS) has attracted much attention in the past decade due to its wide applications in various fields, including analytical chemistry, life science, and medical science.[1−6] For practical application, not only strong enhancement factors but also good stability and reproducibility are required for an efficient SERS substrate.[7,8] Furthermore, to make SERS as a general analytical tool, the fabrication of the SERS substrates should become much cheaper and more easily handled.

The local electromagnetic field enhancement induced by the excitation of the surface plasmon (SP) of the noble metal surface is the major mechanism for SERS.[6] While a metallic nanostructure is illuminated, it can create SERS "hot spots".[9] At these "hot spots", due to the efficient coupling of such a plasmon-induced near field with vibration modes of either molecules adsorbed or crystals attached, the Raman scattering cross section of the adsorbents can be amplified by several orders of magnitude.[10−13] The optical response of a metallic nanoparticle is a sensitive function of its shape, size, and surrounding environment of the nanoparticle.[14,15] Various metallic nanostructures have been fabricated for SERS, including nanoparticles, nanorods, nanocubes, nanotriangles, and core−shell nanoparticles.[16−20] In particular, since the report of the strong SERS enhancement from semiconductor nanostructures recently,[21] more semiconductor−noble metal nanocomposites were fabricated, such as TiO_2/Ag, ZnO/Ag, ZnO/Au, TiO_2/Au, and Si/Ag composites,[22−28] which show evident enhancement.

Aside from the enhancement, the application of SERS as a general analytical tool requires stability or reproducibility. Thus, much efforts have been put in fabricating SERS substrates with better controllability, among which the periodic arrays of metallic nanoparticles is the most common type.[29,30] Particularly, the ordered metallic semishell array possesses favorable features for SERS because of merits as follows: a controllable interparticle distance, a precise control of the symmetry-broken geometry, and uniform orientation of the created nanoapertures.[31−33] The Ag semishell array fabricated by the nanosphere lithography (NSL) has been reported with a strong SERS enhancement and a high reproducibility.[34] However, considering the stability, Au is much more oxidation-resistant than Ag and thus holds an excellent application for SERS.[35] Finally, most of the traditional metal-based SERS substrates cannot be easily reused, which is a serious drawback when considering the preciousness of transition metals. Thus, in recent years, the research has been focused on developing renewable SERS substrates.[35−37] However, the so-far reported reusable SERS substrates are based on either random metal particles[32−34] or particles supported by disordered arrays.[38,39] It is more desirable to fabricate recyclable SERS substrates based on a uniform "Au semishell on TiO_2 structure arrays" in a large-scale ordering, which allows better control in enhancement and reproducibility.

Received: February 2, 2012
Accepted: April 3, 2012
Published: April 3, 2012

dx.doi.org/10.1021/am300189n | *ACS Appl. Mater. Interfaces* 2012, 4, 2180−2185

Here, we report a recyclable SERS-active substrate comprising 2-D ordered arrays of Au semishells on TiO_2 spheres fabricated using all-scalable techniques including nanosphere monolayer self-assembly, atomic layer deposition, and metal evaporation. The Raman enhancement originates from the ordered gold nanogaps, and the recyclability stems from the UV-photocatalytic degradation of the target molecules by the exposed surfaces of the TiO_2 spheres (i.e., self-cleaning). The size of the nanogaps is controlled by the sphere size and ALD thickness (not by gold film thickness which would otherwise block the TiO_2 surface and weakens the self-cleaning function). Sensitivity, reproducibility, and recyclability are demonstrated by Raman detection of three typical molecules.

2. EXPERIMENTAL SECTION

2.1. Fabrication of Au Semishell on TiO_2 Sphere Array. The fabrication process for the ordered array of Au semishell on hollow TiO_2 sphere is illustrated in Figure 1. First, an ordered monolayer of polystyrene (PS) nanospheres (purchased from Polysciences, Inc.) was deposited on a glass substrate using the Langmuir–Blodgett technique as described in the literature.[40,41] The concentration of the PS is 2.61% (w/w), and the size distribution of the PS is 465 ± 10 nm. Second, the as-deposited PS monolayers were etched to a reduced size with a proper interparticle distance using a March PX-250 plasma etching system. A pressure of 70 mtorr, a RF power of 100 W, an O_2 flow rate of 50 sccm (cubic cm per min), and an etching time of 300 s were applied for the reactive ion etching (RIE). After RIE, about 20 nm of TiO_2 were coated on the PS mask by ALD. The ALD was performed on a Beneq TFS-200 system using $TiCl_4$ and deionized water as the Ti and oxygen precursor, respectively.[42] High purity N_2 was the process gas in our experiment. During the deposition, the reaction chamber was maintained at 1.0 mbar with a steady N_2 steam at 200 sccm. Each ALD cycle consisted of a 250 ms precursor pulse and 2 s purging time with N_2. The deposition temperature was chosen as 80 °C to avoid damage of the PS spheres.[43] The growth rate is about 0.06 nm pre cycle, which is inconsistent with the previous report. Subsequently, the substrates were annealed in air ambient at 450 °C to remove the PS sphere and at the meantime to crystallize the TiO_2 layer. Finally, a ~30 nm thick Au layer was deposited on the hollow TiO_2 array by an Edward electron-beam evaporation system.

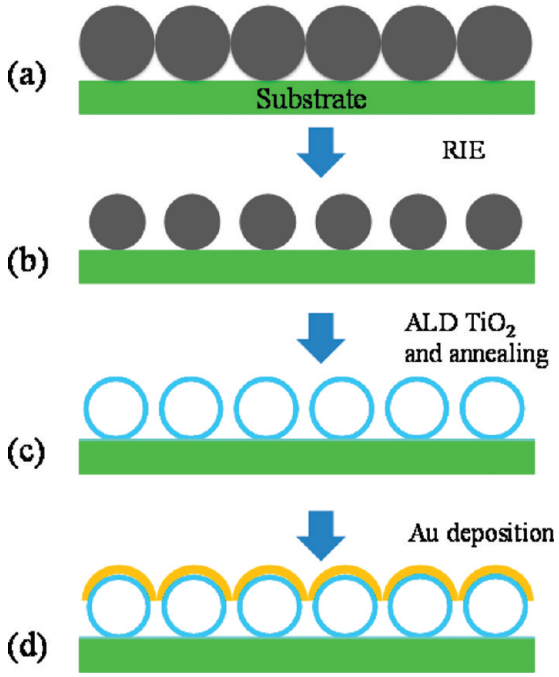

Figure 1. Schematics of the fabrication process of the Au semishell on TiO_2 nanosphere array: (a) deposition of the monolayer PS sphere; (b) shrink of the PS sphere by using RIE; (c) deposition of TiO_2 by ALD and thermal annealing; (d) evaporation of Au on the hollow TiO_2 sphere array.

2.2. SERS Experiments and Self-Cleaning Cycles. The ordered arrays of Au semishell on hollow TiO_2 sphere were used as SERS-active substrates. The substrates were immersed in the prepared target molecular solutions for 30 min and then washed with deionized water and dried by N_2 flow before SERS measurement. We used the Rhodamine 6G (R6G) and brilliant cresyl blue (BCB) as the probe molecules. After samples were studied for SERS with a 785 nm excitation laser, they were immersed in deionized water and irradiated with a 4 W UV lamp (peak wavelength: 254 nm) at room temperature for a certain time (typically 1.5 h for BCB and 2 h for R6G; note that the irradiation time could be shortened by using a higher power UV light source). Then the sample was rinsed with deionized water several times to remove the residual ions and molecules and dried with N_2 flow. For recyclability characterization, the "detection–cleaning" process was repeated five times for each sample.

2.3. Characterizations. The morphology of the ordered arrays of Au semishell on hollow TiO_2 sphere was characterized by a JEOL JSM-6700F field emission scanning electron microscope (FE-SEM). The UV–vis absorption spectra were taken on a microspectrophotometer (Craic 2000). The Raman spectra were collected at room temperature from a Renishaw invia Raman system. A 785 nm laser was used as the excitation source, and the scattered light from the sample was collected in the back scattering geometry. A 50× objective lens was used to focus the laser beam. In all SER measurements, the laser power was fixed to 25 mW, 0.5%, and integration time was 10 s.

3. RESULTS AND DISCUSSION

The fabrication process of the ordered array of Au–TiO_2 composite sphere SERS substrates mainly involves three main steps (see Figure 1). First, a large-area ordered monolayer of polystyrene (PS) nanosphere was deposited on glass substrate. Second, the PS sphere size was reduced by oxygen plasma in order to create enough separation between the spheres for the subsequent ALD and metal deposition. The size of the PS can be controlled by adjusting the RIE etching time when other conditions are fixed.[43] Then a TiO_2 layer was coated on the PS sphere surfaces by ALD. ALD is a cyclic self-limiting deposition method, which is capable of conformal and uniform coating of thin films at the atomic level on high-aspect-ratio templates.[44] The thickness of the TiO_2 is precisely controlled by the ALD cycles. In our experiment, we used 340 cycles to deposit about 20 nm thick TiO_2 film.[45] After ALD, the substrates were annealed at 450 °C for one h at ambient condition to remove the PS. As both the RIE and ALD are controllable processes, the size of the hollow TiO_2 spheres, sphere thickness, and the interparticle distance can be controlled.[46] Finally, about 30 nm of Au film was deposited on the substrate by e-beam evaporator.

Figure 2a shows the SEM image of the etched PS sphere with the initial size 465 nm. After etching, the diameter of PS spheres is reduced to uniform 420 nm. At the same time, the interparticle distance is about 80 nm. Figure 2b shows the hollow TiO_2 sphere array after ALD and thermal annealing. The hexagonal close-packed monolayer hollow TiO_2 spheres have a uniform size of about 440 nm. This demonstrates that a combination of nanosphere patterning, RIE, and ALD provides a useful and powerful technique for preparing uniform micro/nano patterns with controlled particle size and tunable interparticle distance. Parts c and d of Figure 2 show the

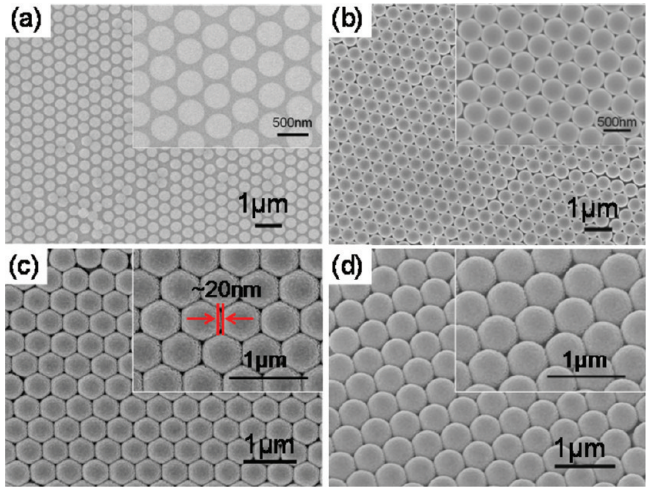

Figure 2. SEM images: (a) PS sphere after the RIE etching; (b) hollow TiO_2 sphere array after ALD and thermal annealing; (c) Au semishell on TiO_2 hollow sphere array obtained by evaporation; (d) tilted image of the structure in (c). The insets show the corresponding larger-magnification SEM images.

SEM image and the 20° tilted SEM image of the ordered array of Au semishells on hollow TiO_2 spheres. The Au films were 30 nm in thickness and homogeneous. After evaporation, both of the interspaces between hollow TiO_2 spheres and the top surface of the hollow TiO_2 sphere were covered with Au. As the diameter of the etched PS sphere is identical, the size of the Au semishell is the same (~500 nm) and the interparticle distance is about 20 nm as indicated by the red maker in Figure 2c. Figure 3a shows the Raman spectrum of the initial ordered array of Au semishells on hollow TiO_2 spheres substrates. The Raman peaks can be assigned as the E_g (143 cm^{-1}), A_{1g} (395 cm^{-1}), or B_{1g} (515 cm^{-1}) and E_g (638 cm^{-1}) modes of the anatase TiO_2 phase, respectively.[47] Except for the Raman peak

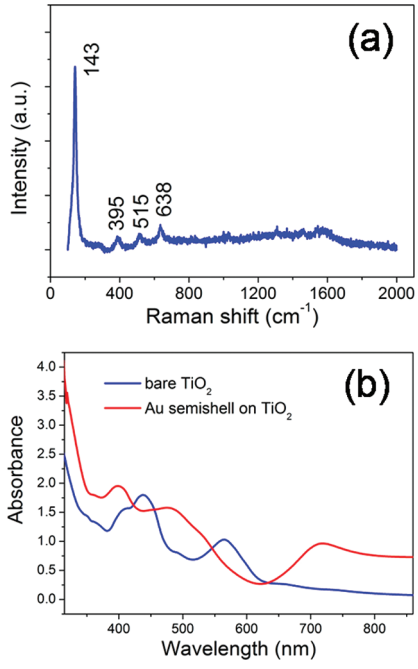

Figure 3. (a) Raman spectrum and (b) UV–vis absorption spectra of the initial Au semishell on TiO_2 hollow sphere array substrates.

at 143 cm^{-1}, all the other peaks are quite low, which means we have a clear background for SERS application.

UV–vis absorption spectra of the ordered array of hollow TiO_2 spheres array before and after Au deposition are shown in Figure 3b. The absorption edge at 380 nm observed for both of the substrates corresponds to the bulk value (3.2 eV) of the TiO_2 band gap. Before Au deposition, two main broad peaks were observed at ~440 and ~560 nm, which are believed to originate from the hexagonal close packing of the spheres.[34,48] There is no absorption peak in the range beyond 600 nm. After Au deposition, the two peaks in the range of 400–600 nm blue-shifted slightly. That may be due to the change of the particles size and surrounding materials.[49] A new broad plasmon band, centered at ~730 nm, appeared, corresponding to the transverse plasmon mode of the Au semishell on the hollow TiO_2 sphere. It is known that for a single semishell, different orientations of electric field generated different plasmon modes, known as the axial mode and the transverse mode.[33,50,51] The energy of the transverse mode is usually lower than axial mode. Because of the overlapping, we cannot observe the axial mode, whereas the transverse mode resonance peak appears clearly at ~730 nm.

The ordered arrays of Au semishells on hollow TiO_2 spheres are used as substrates for the Raman detection of different molecular species. Figure 4 shows the SERS spectra of BCB absorbed on the substrates, with the concentration ranging from 10^{-6} down to 10^{-9} M. Evident Raman detection was obtained from concentration from 10^{-9} M and above. A renewable substrate can be obtained for further detection after it fully cleans itself by TiO_2 photocatalytic degradation of the target molecules adsorbing on the substrates. For BCB and R6G molecules, their photocatalytic degradation in presence of TiO_2 has been studied by Baran et al.[52] The typical self-cleaning process is as follows: after Raman measurement, the substrates were immersed in deionized water with UV light for a certain time and then the sample was rinsed with deionized water to remove the residual ions and molecules and dried with N_2 flow. Figure 4b shows the Raman spectra of BCB adsorbed on the substrate before and after cleaning. After 45 min of UV irradiation, the BCB signal was very weak and it completely vanished after 90 min of UV irradiation. The signal was fully recovered after subsequent soaking of the substrates into the BCB solution, indicating that the substrates preserved their functionality. Figure 5a shows that the result is well reproduced after repeating the "detection–cleaning" procedure five times. In addition to BCB, other types of molecules can be detected repeatedly by the same substrate, for example, the R6G, as shown in Figure 5b. Remarkably, the characteristic vibration patterns can be clearly identified when the analyte is present but are completely eliminated after UV irradiation and washing. These results further demonstrate the general reversibility of such ordered array of Au–TiO_2 spheres for the detection of a variety of organic molecules.

To numerically estimate the electromagnetic field distribution in the structure, a 3D finite-difference time-domain (FDTD) simulation is carried out on a commercial software package (Lumerical FDTD Solution 7.1, Inc., Canada). The model of the structure is shown in Figure 4a, where the particle size is 500 nm and the interparticle distance is 20 nm. The grid was set to a 4.0 nm cubic in our calculation. The Au dielectric constant we used is from Johnson and Christy, and for the TiO_2, the constant we used is from Palik. As our substrate was an ordered array, a periodic boundary condition was used in the

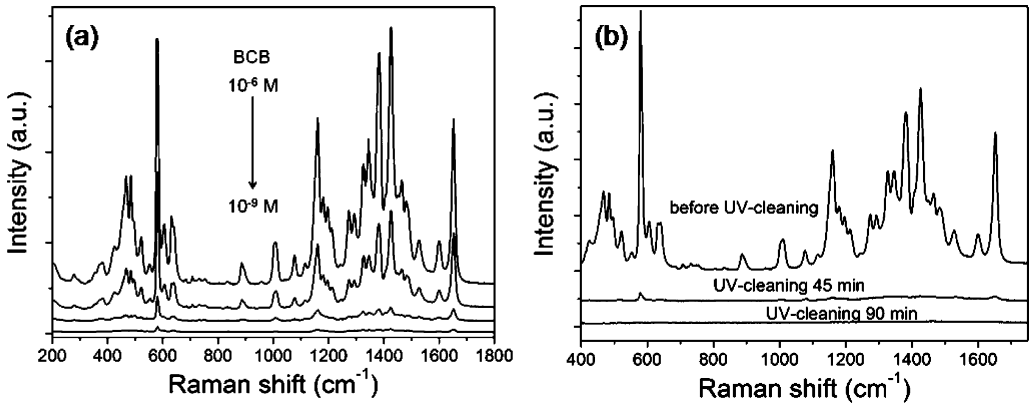

Figure 4. SERS spectra of BCB solutions at different concentrations. From top to bottom: 10^{-6}, 10^{-7}, 10^{-8}, 10^{-9} M. (b) Raman spectra of BCB solution (1×10^{-7} M) adsorbed on the Au semishell on hollow TiO_2 sphere array before and after UV cleaning using 4 W UV lamp.

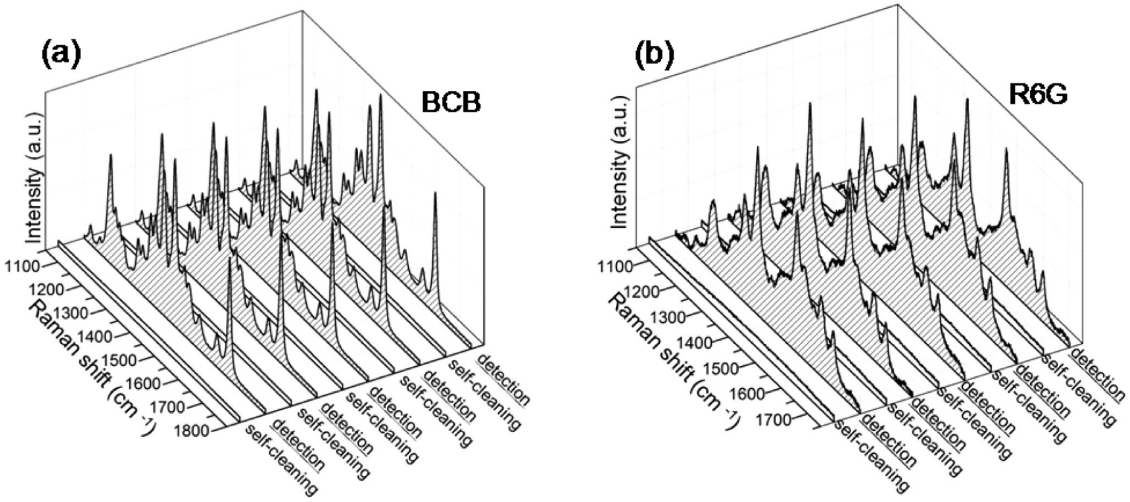

Figure 5. Raman spectra of five adsorption/UV cleaning cycles of (a) BCB 10^{-7} M and (b) R6G 10^{-6} M, respectively. Each cycle consists of adsorption of the target solution followed by UV irradiation. The graph shows the Raman spectra before and after cleaning.

simulation. A 785 nm sinusoidal plane electromagnetic wave with normal incident from the two is chosen in our simulation, as shown in Figure 6a. The simulation results show that the semishells array generates the localized plasmons and substantial electromagnetic field enhancement in the gaps between the semishells, as shown in Figure 6b,c. These gaps are vital hot spots for SERS.

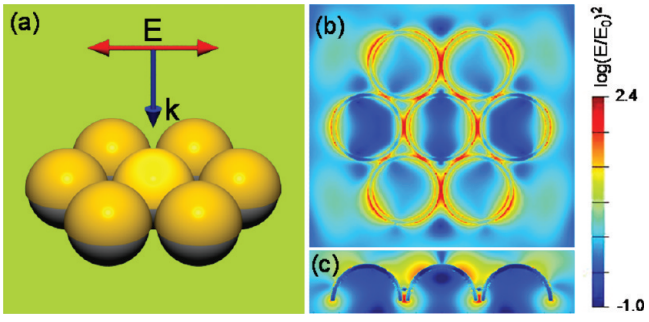

Figure 6. 3D-FDTD simulation of a unit cell of the Au semishell arrays excited at 785 nm: (a) the simulation model; (b) top view of the simulation results; (c) side view of the simulation results. Significant electromagnetic field enhancement is seen in the gaps.

The sensitivity of a SERS substrate is characterized by the enhancement factor (EF). EF is defined by comparing the intensity of the SERS signal with that of the non-SERS signal[53]

$$\mathrm{EF} = (I_{\mathrm{SERS}}/N_{\mathrm{SERS}})/(I_0/N_0) \quad (1)$$

where N_{SERS} and N_0 are the numbers of probe molecules contributing to the SERS signal and non-SERS signal, respectively, and I_{SERS} and I_0 are the intensities of the selected scattering bands in the SERS and non-SERS spectra, respectively (Figure 5). The probed molecules are assumed to distribute on the substrates uniformly. Because the specimens for SERS and non-SERS detection are prepared in the same way except for only the substrate (single crystal Au foil for non-SERS), the number of the detected molecule can be estimated by

$$N = (N_{\mathrm{A}} M V_{\mathrm{solution}}/S_{\mathrm{sub}})S_{\mathrm{laser}} \quad (2)$$

where N_{A} is Avogadro constant, M is the molar concentration of the solution, V_{solution} is the volume of the droplet, S_{sub} is the size of the substrate, and S_{laser} is the size of the laser spot. To prepare the SERS sample, 2 μL of 10^{-6} M R6G solution was dropped on the Au semishells on TiO_2 spheres ordered array substrate with a diameter about 4 mm. For the reference, 2 μL of 10^{-3} M R6G solution was also dropped on a single crystal gold foil for the non-SERS measurements with the diameter

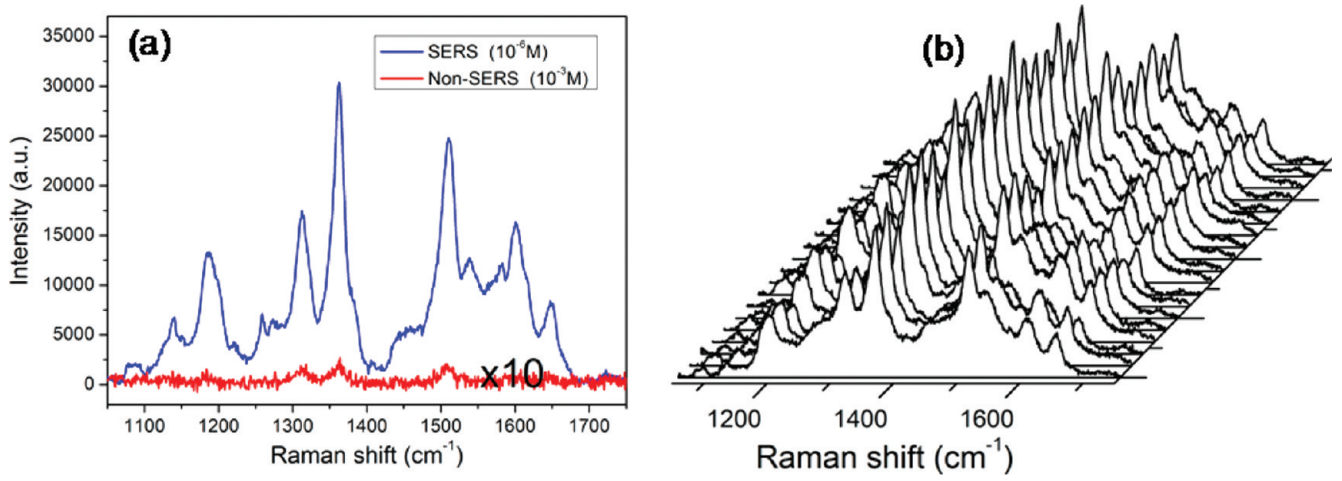

Figure 7. (a) SERS spectra of R6G adsorbed on the ordered Au semishells (blue) on hollow TiO_2 spheres substrate and the single crystal gold foil (red) (excited at 785 nm). (b) SERS spectra of R6G on Au semishell on hollow TiO_2 sphere array substrate from 20 randomly selected places.

about 4 mm. Results of the comparison measurement are shown in Figure 7a, from which and by combining eqs 1 and 2 the average EF of ordered array of Au semishells on TiO_2 spheres was estimated to be 1.4×10^5, which is comparable with the Ag semishells arrays.[34] The characteristic band at 1360 cm^{-1} was chosen for the EF estimation.

In addition to the high sensitivity, the reproducibility of SERS signal is also an important parameter. Usually, nanoparticle aggregates could produce large enhancement, but the signal reproducibility is poor due to the random field distribution.[54] It is expected that the uniform nanostructure, and hence the uniform spatial distribution of the electric field, of an ordered array endow this substrate with improved reproducibility. To test the reproducibility of our sample, SERS spectra of R6G molecules with a concentration of 10^{-6} M from 20 random-selected places on the ordered array of Au semishells on hollow TiO_2 spheres substrate were collected under identical experimental conditions. Figure 7b shows the SERS spectra. For the strongest peak at 1360 cm^{-1}, the relative standard deviation (RSD) of the SERS intensity is about 12%. This low RSD indicates that the structure and surface property of our substrate is rather uniform.

CONCLUSIONS

A facile and new strategy for the creation of recyclable SERS-active substrates has been presented based on the ordered array of Au semishells on hollow TiO_2 spheres. The whole structure is fabricated by nanosphere monolayer assembly, ALD, and metal evaporation; all are scalable techniques with good control. Raman measurements reveal that the ordered array of Au–TiO_2 composite can indeed be a high-performance SERS platform which is highly sensitive (due to nanogaps between the Au semishells), stable, reproducible (uniform arrays), and recyclable (self-cleaning enabled by the UV photocatalytic characteristics of TiO_2). The unique recyclable capability provides a new opportunity in eliminating the single-use problem of traditional SERS substrates and creates promising applications as a functional component in surface-enhanced spectroscopy and quantitative analysis.

AUTHOR INFORMATION

Corresponding Author

*E-mail: fanhj@ntu.edu.sg.

Notes

The authors declare no competing financial interest.

ACKNOWLEDGMENTS

This work is supported by the SPMS Collaboration Award (M58110091) and AcRF Tier 1 grant (M4011011.110).

REFERENCES

(1) Maher, R. C.; Galloway, C. M.; Le Ru, E. C.; Cohena, L. F.; Etchegoin, P. G. *Chem. Soc. Rev.* **2008**, *37* (5), 965–979.
(2) Cao, Y. W. C.; Jin, R. C.; Mirkin, C. A. *Science* **2002**, *297* (5586), 1536–1540.
(3) Porter, M. D.; Lipert, R. J.; Siperko, L. M.; Wang, G.; Narayanana, R. *Chem. Soc. Rev.* **2008**, *37* (5), 1001–1011.
(4) Camden, J. P.; Dieringer, J. A.; Zhao, J.; Van Duyne, R. P. *Acc. Chem. Res.* **2008**, *41* (12), 1653–1661.
(5) Graham, D.; Thompson, D. G.; Smith, W. E.; Faulds, K. *Nature Nanotechnol.* **2008**, *3* (9), 548–551.
(6) Anker, J. N.; Hall, W. P.; Lyandres, O.; Shah, N. C.; Zhao, J.; Van Duyne, R. P. *Nature Mater.* **2008**, *7* (6), 442–453.
(7) Li, W. Y.; Camargo, P. H. C.; Lu, X. M.; Xia, Y. N. *Nano Lett.* **2009**, *9* (1), 485–490.
(8) Zhang, B. H.; Wang, H. S.; Lu, L. H.; Ai, K. L.; Zhang, G.; Cheng, X. L. *Adv. Funct. Mater.* **2008**, *18* (16), 2348–2355.
(9) Chen, T.; Wang, H.; Chen, G.; Wang, Y.; Feng, Y. H.; Teo, W. S.; Wu, T.; Chen, H. Y. *ACS Nano* **2010**, *4* (6), 3087–3094.
(10) Fang, Y.; Seong, N. H.; Dlott, D. D. *Science* **2008**, *321* (5887), 388–392.
(11) Liberman, V.; Yilmaz, C.; Bloomstein, T. M.; Somu, S.; Echegoyen, Y.; Busnaina, A.; Cann, S. G.; Krohn, K. E.; Marchant, M. F.; Rothschild, M. *Adv. Mater.* **2010**, *22* (38), 4298–4302.
(12) Han, X. X.; Huang, G. G.; Zhao, B.; Ozaki, Y. *Anal. Chem.* **2009**, *81* (9), 3329–3333.
(13) Han, X. X.; Jia, H. Y.; Wang, Y. F.; Lu, Z. C.; Wang, C. X.; Xu, W. Q.; Zhao, B.; Ozaki, Y. *Anal. Chem.* **2008**, *80* (8), 2799–2804.
(14) Link, S.; El-Sayed, M. A. *J. Phys. Chem. B* **1999**, *103* (21), 4212–4217.
(15) Halas, N. J. *Nano Lett.* **2010**, *10* (10), 3816–3822.
(16) Smith, W. E. *Chem. Soc. Rev.* **2008**, *37* (5), 955–964.
(17) Shen, C. M.; Hui, C.; Yang, T. Z.; Xiao, C. W.; Tian, J. F.; Bao, L. H.; Chen, S. T.; Ding, H.; Gao, H. J. *Chem. Mater.* **2008**, *20* (22), 6939–6944.
(18) Yoon, I.; Kang, T.; Choi, W.; Kim, J.; Yoo, Y.; Joo, S. W.; Park, Q. H.; Ihee, H.; Kim, B. *J. Am. Chem. Soc.* **2009**, *131* (2), 758–762.
(19) Chen, H. J.; Wang, Y. L.; Dong, S. J. *J. Raman Spectrosc.* **2009**, *40* (9), 1188–1193.

(20) Hu, X. G.; Cheng, W. L.; Wang, T.; Wang, Y. L.; Wang, E. K.; Dong, S. J. *J. Phys. Chem. B* **2005**, *109* (41), 19385−19389.
(21) Musumeci, A.; Gosztola, D.; Schiller, T.; Dimitrijevic, N. M.; Mujica, V.; Martin, D.; Rajh, T. *J. Am. Chem. Soc.* **2009**, *131* (17), 6040−6041.
(22) Yang, L. B.; Jiang, X.; Ruan, W. D.; Yang, J. X.; Zhao, B.; Xu, W. Q.; Lombardi, J. R. *J. Phys. Chem. C* **2009**, *113* (36), 16226−16231.
(23) Cheng, C. W.; Yan, B.; Wong, S. M.; Li, X. L.; Zhou, W. W.; Yu, T.; Shen, Z. X.; Yu, H. Y.; Fan, H. J. *ACS Appl. Mater. Interfaces* **2010**, *2* (7), 1824−1828.
(24) Wang, X. T.; Shi, W. S.; She, G. W.; Mu, L. X.; Lee, S. T. *Appl. Phys. Lett.* **2010**, *96* (5), 053104−053107.
(25) Deng, S.; Fan, H. M.; Zhang, X.; Loh, K. P.; Cheng, C. L.; Sow, C. H.; Foo, Y. L. *Nanotechnology* **2009**, *20* (17), 175705−175712.
(26) Alessandri, I. *J. Colloid Interface Sci.* **2010**, *351* (2), 576−579.
(27) Alessandri, I.; Depero, L. E. *Chem. Commun.* **2009**, *17*, 2359−2361.
(28) Alessandri, I.; Ferroni, M.; Depero, L. E. *ChemPhysChem* **2009**, *10* (7), 1017−1022.
(29) Liao, Q.; Mu, C.; Xu, D.-S.; Ai, X.-C.; Yao, J.-N.; Zhang, J.-P. *Langmuir* **2009**, *25* (8), 4708−4714.
(30) Li, J. F.; Huang, Y. F.; Ding, Y.; Yang, Z. L.; Li, S. B.; Zhou, X. S.; Fan, F. R.; Zhang, W.; Zhou, Z. Y.; Wu, D. Y.; Ren, B.; Wang, Z. L.; Tian, Z. Q. *Nature* **2010**, *464* (7287), 392−395.
(31) Ye, J.; Van Dorpe, P.; Van Roy, W.; Lodewijks, K.; De Vlaminck, I.; Maes, G.; Borghs, G. *J. Phys. Chem. C* **2009**, *113* (8), 3110−3115.
(32) Ye, J. A.; Chen, C.; Lagae, L.; Maes, G.; Borghs, G.; Van Dorpe, P. *Phys. Chem. Chem. Phys.* **2010**, *12* (37), 11222−11224.
(33) Ye, J.; Verellen, N.; Van Roy, W.; Lagae, L.; Maes, G.; Borghs, G.; Van Dorpe, P. *ACS Nano* **2010**, *4* (3), 1457−1464.
(34) Wang, C. X.; Ruan, W. D.; Ji, N.; Ji, W.; Lv, S.; Zhao, C.; Zhao, B. *J. Phys. Chem. C* **2010**, *114* (7), 2886−2890.
(35) Wang, T.; Hu, X. G.; Dong, S. J. *Small* **2008**, *4* (6), 781−786.
(36) Li, M.-D.; Cui, Y.; Gao, M.-X.; Luo, J.; Ren, B.; Tian, Z.-Q. *Anal. Chem.* **2008**, *80* (13), 5118−5125.
(37) Aldeanueva-Potel, P.; Faoucher, E.; Alvarez-Puebla, R. A.; Liz-Marzan, L. M.; Brust, M. *Anal. Chem.* **2009**, *81* (22), 9233−9238.
(38) Sinha, G.; Depero, L. E.; Alessandri, I. *ACS Appl. Mater. Interfaces* **2011**, *3* (7), 2557−2563.
(39) Li, X. H.; Chen, G. Y.; Yang, L. B.; Jin, Z.; Liu, J. H. *Adv. Funct. Mater.* **2010**, *20* (17), 2815−2824.
(40) Kosiorek, A.; Kandulski, W.; Chudzinski, P.; Kempa, K.; Giersig, M. *Nano Lett.* **2004**, *4* (7), 1359−1363.
(41) Zhang, J. H.; Li, Y. F.; Zhang, X. M.; Yang, B. *Adv. Mater.* **2010**, *22* (38), 4249−4269.
(42) Li, X. L.; Li, C.; Zhang, Y.; Chu, D. P.; Milne, W. I.; Fan, H. J. *Nanoscale Res. Lett.* **2010**, *5* (11), 1836−1840.
(43) Cong, C. X.; Junus, W. C.; Shen, Z. X.; Yu, T. *Nanoscale Res. Lett.* **2009**, *4* (11), 1324−1328.
(44) Knez, M.; Niesch, K.; Niinisto, L. *Adv. Mater.* **2007**, *19* (21), 3425−3438.
(45) Wang, X. D.; Lao, C. S.; Graugnard, E.; Summers, C. J.; Wang, Z. L. *Nano Lett.* **2005**, *5* (9), 1784−1788.
(46) Cheng, C. W.; Karuturi, S. K.; Liu, L. J.; Liu, J. P.; Li, H. X.; Su, L. T.; Tok, A. I. Y.; Fan, H. J. *Small* **2012**, *8* (1), 37−42.
(47) Li, Q. J.; Liu, B. B.; Li, Y. G.; Liu, R.; Li, X. L.; Li, D. M.; Yu, S. D.; Liu, D. D.; Wang, P.; Li, B.; Zou, B.; Cui, T.; Zou, G. T. *J. Alloys Compd.* **2009**, *471* (1−2), 477−480.
(48) Liu, L.; Karuturi, S. K.; Su, L. T.; Tok, A. I. Y. *Energy Environ. Sci.* **2011**, *4* (1), 209−215.
(49) Maaroof, A. L.; Cortie, M. B.; Harris, N.; Wieczorek, L. *Small* **2008**, *4* (12), 2292−2299.
(50) Cortie, M.; Ford, M. *Nanotechnology* **2007**, *18* (23), 235704−235710.
(51) King, N. S.; Li, Y.; Ayala-Orozco, C.; Brannan, T.; Nordlander, P.; Halas, N. J. *ACS Nano* **2011**, *5* (9), 7254−7262.
(52) Baran, W.; Makowski, A.; Wardas, W. *Dyes Pigm.* **2008**, *76* (1), 226−230.
(53) Le Ru, E. C.; Blackie, E.; Meyer, M.; Etchegoin, P. G. *J. Phys. Chem. C* **2007**, *111* (37), 13794−13803.
(54) Suzuki, M.; Niidome, Y.; Kuwahara, Y.; Terasaki, N.; Inoue, K.; Yamada, S. *J. Phys. Chem. B* **2004**, *108* (31), 11660−11665.